



## Modification of CeO<sub>2</sub>-ZrO<sub>2</sub> catalyst by potassium for NO<sub>x</sub>-assisted soot oxidation

Duan Weng\*, Jia Li, Xiaodong Wu, Zhichun Si

State Key Laboratory of New Ceramics & Fine Process, Department of Materials Science and Engineering, Tsinghua University, Beijing 100084, China. E-mail: [duanweng@tsinghua.edu.cn](mailto:duanweng@tsinghua.edu.cn)

Received 08 March 2010; revised 29 April 2010; accepted 04 May 2010

### Abstract

Potassium-modified ceria-zirconia catalyst was synthesized by wetness impregnation method. The ageing treatment was performed in static air at 800°C for 20 hr to evaluate the thermal stability of the catalyst. The catalysts were characterized by X-ray diffraction, BET surface area, oxygen storage capacity, NO<sub>x</sub>-temperature programmed desorption and soot-temperature programmed oxidation measurements. By introduction of potassium, the maximum soot oxidation rate temperature ( $T_m$ ) of the ceria-zirconia based catalyst decreased from 525 to 428°C in the presence of NO under a loose contact mode. The shift of  $T_m$  of the K-modified catalyst after ageing is only 15°C. The enhanced activity of the aged catalyst mainly lies in the promotional effect of potassium on the NO<sub>x</sub>/oxygen storage capacity as well as the soot-catalyst contact.

**Key words:** CeO<sub>2</sub>-ZrO<sub>2</sub> mixed oxides; potassium; soot combustion; NO<sub>x</sub> storage; oxygen storage capacity

**DOI:** 10.1016/S1001-0742(10)60386-5

**Citation:** Weng D, Li J, Wu X D, Si Z C, 2011. Modification of CeO<sub>2</sub>-ZrO<sub>2</sub> catalyst by potassium for NO<sub>x</sub>-assisted soot oxidation. *Journal of Environmental Sciences*, 23(1): 145–150.

### Introduction

Diesel engines are more preferable for heavy-duty applications and light-duty trucks due to its superior fuel economy, relatively low pollution emission and high durability compared to gasoline engines. They generally function in a lean burn condition with the air/fuel ratio higher than 20, resulting in relatively low combustion temperatures and lower emissions of HC, CO and CO<sub>2</sub>. However, even the most recent diesel engines generate carcinogenic particulate matters (PM) and harmful NO<sub>x</sub>, which should call for attention because of their environmental aspects. Researchers have found out that these particulates can penetrate the cell membranes, enter the blood, and some may even induce inheritable mutations. A promising alternative is the development of filters which combines filtration and oxidation of PM. The collected soot particles are continuously catalyzed by catalysts or periodically oxidized at higher temperature. Various catalyst systems based on metal oxides, including transition metals such as Co, Ni, Cu and Fe (Zou et al., 2009; Nejar et al., 2005; Neri et al., 2005), rare earth metals such as La, Ce and Pr (Wang et al., 2008; Russo et al., 2005; Bueno-López et al., 2005) and perovskite- and spinel-type oxides (Zhang et al., 2009; Fino et al., 2006), have been widely investigated.

Significant enhancements for soot oxidation can be obtained by adding alkali and alkaline-earth metal salts (Martin et al., 2009; Peralta et al., 2006; Zhang et al., 2006). The predominance of potassium can be attributed to the following factors: (1) the low melting points of the potassium compounds (such as KOH and KNO<sub>3</sub>) or eutectics with other catalytic components, thus enhancing catalyst-soot contact; (2) acting as an electron donor preserving the reducibility and dispersion of transition metals; (3) trapping and releasing gaseous NO<sub>x</sub> involved for soot oxidation; and (4) providing a route for CO<sub>2</sub> release by formation of intermediate carbonates (Wang et al., 2008; Liu et al., 2002; Jiménez et al., 2006). However, their relatively low thermal stability leads to restrained applications in practical systems (Van et al., 2000; Mul et al., 1995). To reinforce the holding capacity of the support is one of effective ways to enhance the thermal stability of such K-containing catalysts.

CeO<sub>2</sub> and CeO<sub>2</sub>-based mixed oxides, which can increase soot oxidation rate by involving the participation of active oxygen, have gained more attention in recent years (Peralta et al., 2006; Zhang et al., 2006; Bueno-López et al., 2005). The oxidation of soot probably involves a redox mechanism in which soot is oxidized by the surface active oxygen from the catalyst which is then reoxidized by the gas phase oxygen (Mckee, 1987; Mul et al., 1998). The redox cycle on such ceria-based catalysts is easy to

\* Corresponding author. E-mail: [duanweng@tsinghua.edu.cn](mailto:duanweng@tsinghua.edu.cn)

occur because the  $Ce^{4+} \longleftrightarrow Ce^{3+}$  change between different oxidation states is available. The loading of potassium can improve the oxygen exchange rate of  $CeO_2$ -based catalysts via a so-called synergistic effect (Liu et al., 2005). In our previous work,  $CeO_2$ ,  $ZrO_2$  and  $Ce_{0.5}Zr_{0.5}O_2$  have been investigated as the potassium carriers (Wu et al., 2007) and the last one is found with more active oxygen and high thermal stability. In the present work, potassium was impregnated to the ceria-zirconia mixed oxides to improve the soot oxidation activity. Especially, the utilization of  $NO_x$  for soot oxidation is elucidated with preliminary studies on structural characterizations,  $NO_x$ -TPD and  $NO$ -TPO tests.

## 1 Experimental

### 1.1 Catalysts preparation

The solution of  $Ce(NO_3)_3 \cdot 6H_2O$  and  $Zr(NO_3)_4 \cdot H_2O$  according to the molar ratio of  $Ce:Zr=1:1$  was added dropwise to ammonia solution, which contained hydrogen peroxide and ammonia in distilled water according to the volume ratio of 1:4:4. The pH of the mixed solution was kept at 10 to ensure the complete precipitation of  $CeO_2$ - $ZrO_2$  mixed oxides. Then the precipitate was filtrated, dried, and calcined in static air at  $500^\circ C$  for 3 hr to obtain the mixed oxides sample (CZ). The as-received CZ support was impregnated with corresponding amount of  $KNO_3$  solution followed by calcination at  $500^\circ C$  for 3 hr to obtain the potassium-containing sample (KCZ). The optimized potassium loading amount of 8 wt.% was adopted according to the reported optimal  $K/C_e$  distribution ratio (Peralta et al., 2006), considering that the doping of  $Zr^{4+}$  into  $Ce^{4+}$  lattice may cause some difference in catalytic properties.

The as-prepared powders are referred to as the fresh samples. In order to simulate the lifetime assessment, an ageing treatment was carried out in static air at  $800^\circ C$  for 20 hr to obtain the aged samples.

### 1.2 Soot combustion measurements

The activities for soot oxidation were evaluated in a temperature-programmed oxidation (TPO) reaction apparatus. The catalyst was mixed with soot (Printex-U, Degussa) following a weight ratio of 10:1 using a spatula for 2 min to produce a loose contact mode, which was more comparable to practical application. The mixture of 110 mg was packed between two quartz wool plugged in a tubular quartz reactor. Then the TPO experiment was carried out at a heating rate of  $20^\circ C/min$  from room temperature (RT) to  $650^\circ C$  in 10%  $O_2/N_2$  or 1000 ppm  $NO/10\% O_2/N_2$  (500 mL/min). Concentrations of  $CO_2$  and  $CO$  in the outlet gases were determined on-line by a five-component analyzer FGA4015 (Foshan Analytical Instrument Co., Ltd., China) equipped with infrared sensor. Repeated experiments was performed to testify the reproducibility of the working system, and the difference between the maximum soot oxidation rate temperature ( $T_m$ ) was within  $10^\circ C$ .

### 1.3 Catalysts characterization

The structural features were determined by powder X-ray diffraction (XRD) using a Japan Science D/max-RB diffractometer employing  $Cu K_\alpha$  radiation ( $\lambda = 0.15418$  nm) combined with a Niche filter operating at 40 kV and 120 mA. The diffractogram was recorded at  $0.02^\circ$  intervals in the range of  $20^\circ \leq 2\theta \leq 85^\circ$  with a scanning velocity of  $4^\circ/min$ . The phase was identified with the help of JCPDS cards (Joint Committee on Powder Diffraction Standards). The average crystallite size and lattice constant of the sample were determined by XRDTHX software using the peak data obtained based on the obtained diffractogram.

The X-ray photoelectron spectroscopy (XPS) experiments were carried out on a PHI-Quantera SXM system equipped with a monochromatic  $Al K_\alpha$  X-rays under UHV ( $6.7 \times 10^{-8}$  Pa). The XPS data from the regions related to the Ce 3d, K 2p, O 1s and Zr 3d core levels were recorded for each sample. The binding energies were calibrated internally by the carbon deposit C 1s binding energy (BE) at 284.8 eV.

The specific surface area was determined by Brunauer-Emmett-Teller (BET) method with a Quantachrome NOVA instrument using Ar as the carrier and  $N_2$  as the adsorbent.

The  $NO_x$  temperature-programmed desorption (TPD) was executed in a fixed-bed reactor with the effluent gaseous monitor using Nicolet Nexus 380 spectrometer (UK), equipped with a gas chamber and a high sensitivity MCT detector cooled by liquid nitrogen. Prior to the TPD experiment, 200 mg of the sample was pretreated in 1000 ppm  $NO/10\% O_2/N_2$  with a total flow rate of 100 mL/min at  $400^\circ C$  for 30 min. Then the reactor was cooled down to RT and then flushed by 100 mL/min  $N_2$  at RT for 30 min.  $NO_2$  and  $NO$  production during the experiment were monitored by 380 spectrometer at a heating rate of  $10^\circ C/min$  to  $600^\circ C$  in a  $N_2$  stream.

$NO$  temperature-programmed oxidation (TPO) was executed using the same apparatus. The experimental runs were performed in a gas mixture of 1000 ppm  $NO/10\% O_2/N_2$  (500 mL/min) at a heating rate of  $10^\circ C/min$  from RT to  $600^\circ C$ .

The oxygen storage capacity (OSC) measurement was performed at  $500^\circ C$  when 4%  $CO/ (1\% Ar/He)$  and  $O_2/ (1\% Ar/He)$  at a total flow rate of 300 mL/min were alternately injected for 5 sec, meaning a test frequency of 0.1 Hz. The OSC of the catalyst was quantified in terms of micromole  $CO_2$  per gram catalyst ( $\mu mol CO_2/g$ ). Before each test, samples (typically 25 mg, mixed with 40 mg quartz) were oxidized in  $O_2/ (1\% Ar/He)$  for 5 min and then purged by pure He for 5 min. The concentrations of outlet gas were detected using an online quadruple mass spectrometer (Omnistar 200, Balzers, Switzerland).

## 2 Results and discussion

### 2.1 Solid properties

The XRD patterns of the fresh and aged catalysts are shown in Fig. 1. All the samples present the characteristic peaks of a fluorite-like cubic ceria phase. The XPS results

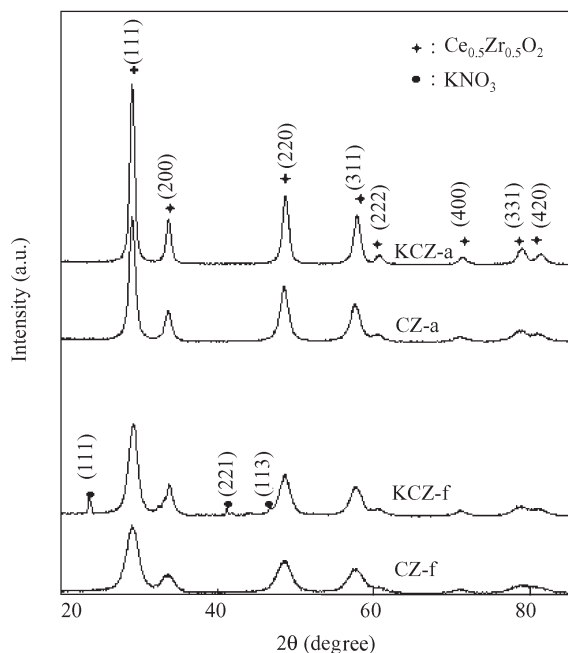


**Fig. 1** XRD patterns of the fresh (f) and aged (a) catalysts.

show that KCZ-a catalyst maintains 6.2 wt.% of K<sup>+</sup> on the surface compared with that of 8.6 wt.% on KCZ-f. It indicates a quite strong ability of this catalyst for holding potassium during the ageing treatment at 800°C. Typical peaks of potassium nitrate are observed in KCZ-f, which disappear after ageing arising from decomposition

or evaporation of KNO<sub>3</sub> (Meijer et al., 1991). Despite the volatile nature of such active component, the encapsulation of K species by other phases or the disability of the XRD method to detect some K-related phases like K-O species should be considered (Krishna and Makkee, 2006). The sharpened and intensified peaks of ceria in KCZ indicate a better crystallization of the catalyst, which is mainly attributed to the additional calcination at 500°C after impregnation with potassium nitrate.

The BET surface areas, lattice constants and average crystallite sizes of the catalysts are summarized in Table 1. It is seen that the loading of potassium had no obvious effect on the lattice constant of the support. The specific surface area of CZ decreases after the impregnation with KNO<sub>3</sub> and subsequent calcination. Micropores of the support can be plugged by the potassium salt to a large extent (Peralta et al., 2006), which is an important reason for the reduced surface area of KCZ.

## 2.2 Catalysts activity for soot combustion

The evolutions of NO, NO<sub>2</sub> and CO<sub>2</sub> concentrations during soot-TPO experiments over KCZ-f and KCZ-a catalysts in different inlet gases are presented in Figs. 2 and 3, respectively. The CO<sub>2</sub> profile of KCZ-f generally exhibits a sharp peak around 430–440°C, indicating a high combustion rate compared with the relatively broadened peak shapes obtained over the aged catalyst. The *T<sub>m</sub>* values and selectivity of the catalysts are listed in Table 2. A drastic decrease in soot combustion temperature is is

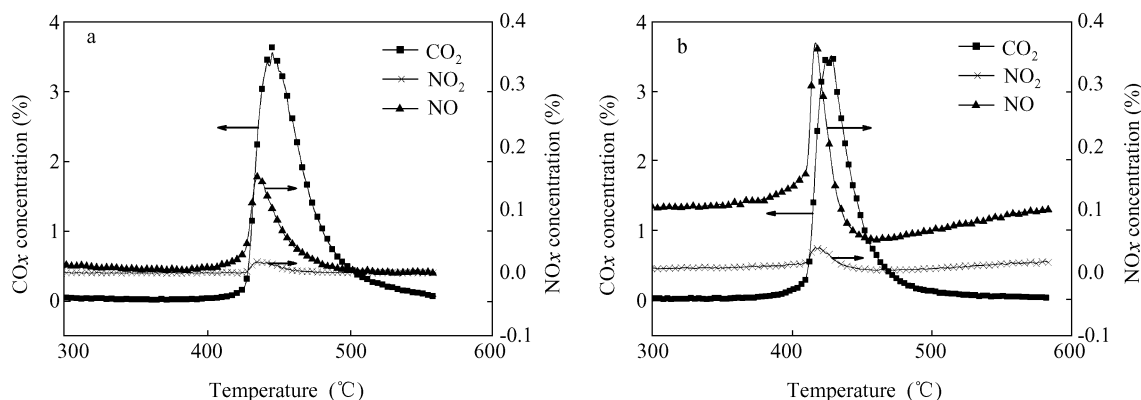


**Fig. 2** NO, O<sub>2</sub> and CO<sub>2</sub> outlet concentration profiles in TPO runs with KCZ-f in O<sub>2</sub> (a) and NO/O<sub>2</sub> (b).

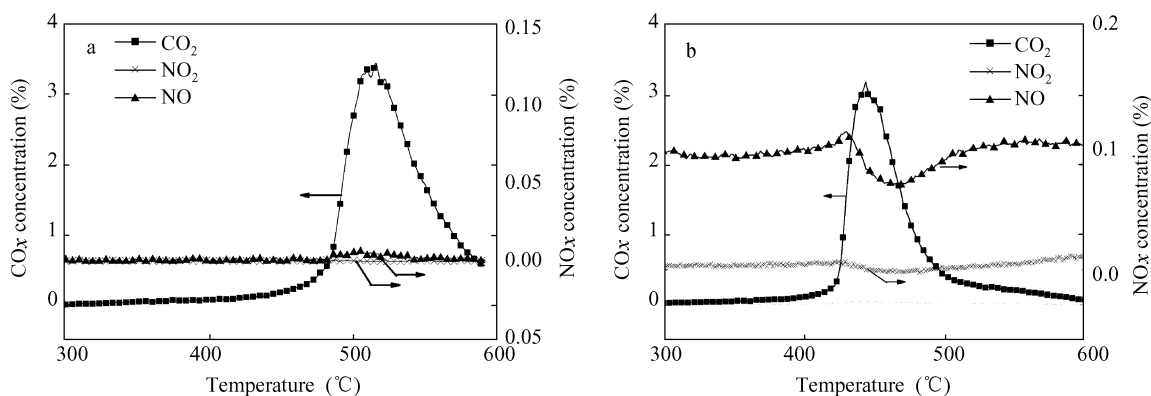


**Fig. 3** NO, O<sub>2</sub> and CO<sub>2</sub> outlet concentration profiles in TPO runs with KCZ-a in O<sub>2</sub> (a) and NO/O<sub>2</sub> (b).

**Table 1** Structural information of the catalysts

Catalyst	BET surface area (m <sup>2</sup> /g)	Lattice constant (nm)	Average crystallite size (nm)
KCZ-f	17	0.5301	7.5
KCZ-a	14	0.5296	19.7
CZ-f	92	0.5306	4.7
CZ-a	32	0.5291	16.4

**Table 2** Relationship between maximum soot oxidation rate temperature ( $T_m$ ) and selectivity ( $S$ ) of the catalysts

Catalyst	NO/O <sub>2</sub>		O <sub>2</sub>	
	$T_m$ (°C)	$S_{CO_2}^*$ (%)	$T_m$ (°C)	$S_{CO_2}^*$ (%)
KCZ-f	428	99	445	99
KCZ-a	443	98	515	97
CZ-f	525	92	545	88
CZ-a	540	84	568	83

\* Calculated by  $C_{CO_2}/(C_{CO} + C_{CO_2})$  in the outlet gas.

observed for the potassium-modified catalyst. Compared with CZ, the shift of  $T_m$  toward lower temperatures over the KCZ-f catalyst is 97 and 100°C in NO/O<sub>2</sub> and O<sub>2</sub> atmosphere, respectively. The difference of  $T_m$  in different reactant gases is about 20–30°C for the CZ-f, CZ-a and KCZ-f catalysts, which illustrates a limited utilization of NO. Contrarily, the KCZ-a catalyst achieves a decrease of  $T_m$  by 72°C with the introduction of NO to the reaction atmosphere.

The enhanced activity of KCZ-f in respect to CZ-f in both atmospheres relies to a great extent on the improvement of the poor catalyst-soot contact. As reported by Teraoka et al. (2001), the migration of the active component across soot surface plays an important role in a loose contact reaction, which can be improved pronouncedly by adding potassium. Corresponding, the loss of potassium nitrate may account mainly for the inevitable but acceptable loss of activity of the aged catalyst in the presence of O<sub>2</sub>. After ageing treatment, the thermodynamically favored utilization of gaseous NO becomes the more predominant factor accounting for the improved activity of KCZ-a under NO/O<sub>2</sub>.

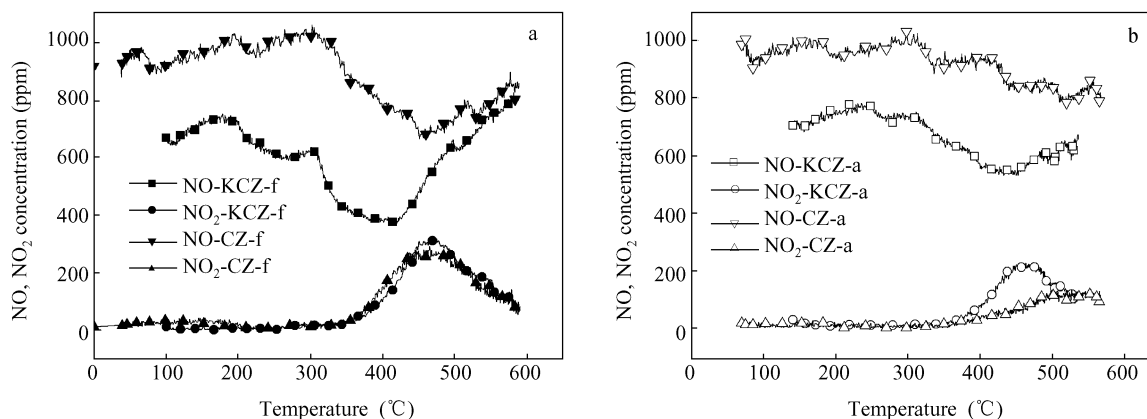
The selectivity of CO<sub>2</sub> in the products for the potassium-loading catalyst is above 97%, while that of CZ catalysts is mostly around 80%–90%. The lower selectivity of the

mixed oxide catalyst may be ascribed to the limited mass transfer under a poor contact mode. The introduction of potassium enhances the transfer of active oxygen species from the oxide catalyst to soot by improving the contact between soot and catalyst, resulting in enhanced selectivity of the catalyst.

It is observed from Figs. 2 and 3 that a sharp NO peak appears simultaneously with the ignition of soot. In the presence of O<sub>2</sub>, the released NO peak of the fresh sample is ascribed to the decomposition of KNO<sub>3</sub> which releases NO<sub>x</sub> to react with soot. Only a trace amount of NO is released over the aged catalyst in O<sub>2</sub>, which confirms the volatilization of potassium during ageing. In the presence of NO, a slip of NO<sub>x</sub> during soot combustion still indicates an effective utilization of gaseous NO over the KCZ-a catalyst. No obvious fluctuates in the NO<sub>x</sub> concentrations are observed over the CZ samples (data not shown), which is in good accordance with the activity results.

### 2.3 NO-TPO and NO<sub>x</sub>-TPD experiment

The beneficial effect of NO<sub>x</sub> on soot combustion is suggested to be ascribed to the formation of NO<sub>2</sub> by oxidation of gaseous NO and decomposition of nitrate, which subsequently reacts with soot and generates NO or N<sub>2</sub>O and N<sub>2</sub> to a much less extent. Figure 4 shows the NO oxidation ability of the catalysts. As shown in Fig. 4a, the fresh CZ and KCZ catalysts behave a similar ability to oxidize NO to NO<sub>2</sub>. However, the difference of NO concentration on two catalysts demonstrates that the NO<sub>x</sub> adsorption mainly relies on the potassium component and the oxidation ability of the mixed oxides. The stored nitrates are stable at temperature as high as 350°C. The oxidation ability is attributed to the ceria-zirconia support with the supply of active oxygen, by which the NO species is more easily captured other than by gaseous O<sub>2</sub>. It should be noted that the TPO runs were performed in N<sub>2</sub>. Thus, it is reasonable to speculate that more NO<sub>2</sub> would be produced by decomposition of the stored nitrates on KCZ-f than CZ-f in excess O<sub>2</sub>. Similar conclusions are obtained for the aged catalysts. Noticeably, the higher amount of NO<sub>2</sub> production over the KCZ-a catalyst implies an improved performance in NO oxidation ability in respect to CZ-a.

**Fig. 4** NO temperature-programmed oxidation curves of fresh (a) and aged catalysts (b).

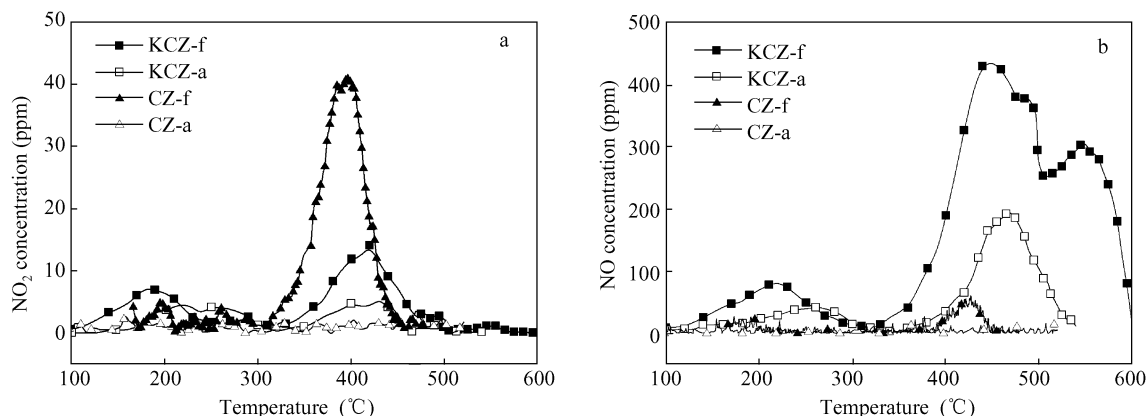


Fig. 5 NO<sub>x</sub>-TPD curves over the fresh and aged catalysts. (a) NO<sub>2</sub> concentration; (b) NO concentration.

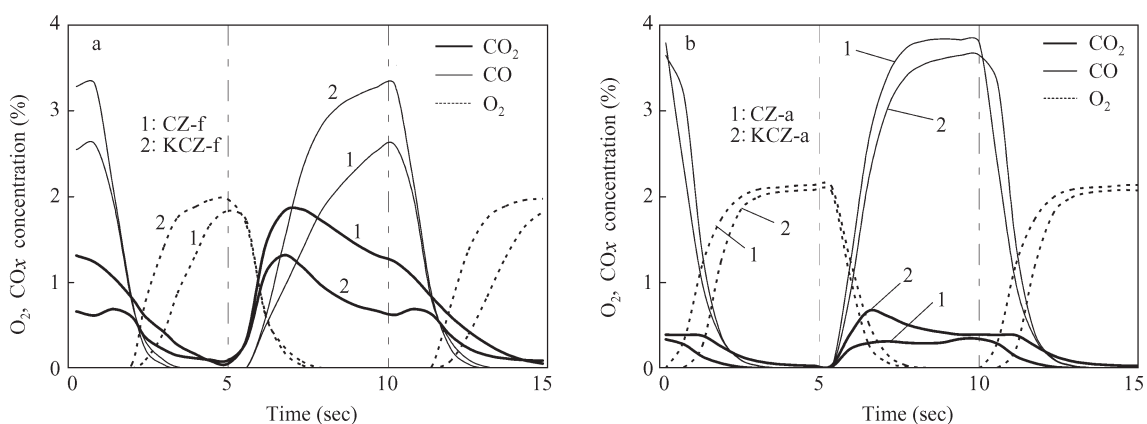


Fig. 6 Curves of CO<sub>x</sub> and O<sub>2</sub> evolutions during CO-O<sub>2</sub> cycle at 500°C under 0.1 Hz over (a) fresh and (b) aged catalysts.

The NO<sub>x</sub>-TPD curves of the catalysts after NO preadsorption at 400°C are shown in Fig. 5. The KCZ-f catalyst exhibits the maximal NO desorption during the catalyst investigated. According to the quite low amount of NO desorbed with a maximal concentration of around 50 ppm, the NO adsorption ability of CZ-f is proved to be poor although the equivalent amounts of NO and NO<sub>2</sub> predict a relatively high NO oxidation ability. After ageing, almost no NO<sub>x</sub> is desorbed from CZ-a while the potassium catalyst maintains a certain NO<sub>x</sub> storage capacity after ageing treatment.

#### 2.4 OSC properties

In our previous works (Liang et al., 2008; Zhu et al., 2007), the OSC has been proven to be an important feature of soot combustion catalysts. Firstly, the active oxygen transfer across soot surface is suggested to be a key issue for soot oxidation activity (Mckee, 1987); secondly, the OSC properties of catalysts provide continuous active oxygen supply in the micro-environments short of O<sub>2</sub> which inevitably exist in diesel exhaust, e.g. in the inner space of the filter cake or the agglomerate bulk of soot-catalysts mixture.

The active oxygen species in a model catalyst can be defined as the amount of CO<sub>2</sub> produced by alternating CO/O<sub>2</sub> pulses (dynamic mode), which is referred to as the

dynamic oxygen storage capacity (DOSC). Figure 6 shows the CO<sub>x</sub> and O<sub>2</sub> concentrations in this mode. The CZ-f catalyst exhibits the largest CO<sub>2</sub> production under alternating conditions, which is weakened to some extent by the modification of potassium. The calculated OSC values of KCZ-f and KCZ-a are 109 and 56 μmol/g, respectively. After ageing, the pure mixed oxides experience a severe loss of OSC from 130 to 31 μmol/g. Thus, the addition of potassium seems to prevent the OSC deterioration to some extent, which is in accordance with the results found in K-promoted vanadium oxide catalysts (Liu et al., 2005). This effect is mainly ascribed to the electron-donating effect of the alkali metal which enhances the reactivity of Ce-O bonds.

### 3 Conclusions

The potassium-modified soot oxidation catalyst synthesized by impregnation exhibits an excellent soot oxidation activity with a decrease of over 100°C in  $T_m$  compared with pure CZ mixed oxides. The utilization of NO by CZ is generally limited by the poor ability to adsorb NO. The introduction of the potassium component improves the NO<sub>x</sub> adsorption behavior and maintains a good OSC of the CZ support against the thermal ageing, resulting in an enhanced catalytic activity compared to the aged CZ.

## Acknowledgments

This work was supported by the Ministry of Science and Technology, China (No. 2009AA064801, 2010CB732304).

## References

- Bueno-López A, Krishna K, Makkee M, Moulijn J A, 2005. Active oxygen from CeO<sub>2</sub> and its role in catalyzed soot oxidation. *Catalysis Letters*, 99: 203–205.
- Bueno-López A, Krishna K, Makkee M, Moulijn J A, 2005. Enhanced soot oxidation by lattice oxygen via La<sup>3+</sup>-doped CeO<sub>2</sub>. *Journal of Catalysis*, 230: 237–248.
- Fino D, Russo N, Saracco G, Specchia V, 2006. Catalytic removal of NO<sub>x</sub> and diesel soot over nanostructured spinel-type oxides. *Journal of Catalysis*, 242: 38–47.
- Jiménez R, García X, Cellier C, Ruiz P, Gordon A L, 2006. Soot combustion with K/MgO as catalyst: II. Effect of K-precursor. *Applied Catalysis A: General*, 314: 81–88.
- Krishna K, Makkee M, 2006. Preparation of Fe-ZSM-5 with enhanced activity and stability for SCR of NO<sub>x</sub>. *Catalysis Today*, 114: 23–30.
- Liang Q, Wu X D, Weng D, Xu H B, 2008. Oxygen activation on Cu/Mn-Ce mixed oxides and the role in diesel soot oxidation. *Catalysis Today*, 139: 113–118.
- Liu J, Zhao Z, Xu C, Duan A J, Zhu L, Wang X Z, 2005. Diesel soot oxidation over supported vanadium oxide and K-promoted vanadium oxide catalysts. *Applied Catalysis B: Environmental*, 61: 36–46.
- Liu Z M, Hao Z P, Guo Y, Zhuang Y H, 2002. Simultaneous catalytic removal of NO<sub>x</sub> and diesel soot particulate over perovskite-type oxides and supported Ag catalyst. *Journal of Environmental Sciences*, 14: 289–295.
- Martin S G, Maria A U, Carlos A Q, 2009. Catalytic oxidation of diesel soot: New characterization and kinetic evidence related to the reaction mechanism on K/CeO<sub>2</sub> catalyst. *Applied Catalysis A: General*, 360: 81–88.
- Mckee D W, 1987. The effects of particulate oxides of the group IIIB elements on oxidation rates of graphite in air. *Journal of Catalysis*, 108: 480–483.
- Meijer R, Weeda M, Kapteijn F, Moulijn J A, 1991. Catalyst loss and retention during alkali-catalysed carbon gasification in CO<sub>2</sub>. *Carbon*, 29: 929–941.
- Mul G, Kapteijn F, Doornkamp C, Moulijn J A, 1998. Transition metal oxide catalyzed carbon black oxidation: A study with <sup>18</sup>O<sub>2</sub>. *Journal of Catalysis*, 179: 258–266.
- Mul G, Neeft J P A, Kapteijn F, Makkee M, 1995. Soot oxidation catalyzed by a Cu/K/Mo/Cl catalyst: evaluation of the chemistry and performance of the catalyst. *Applied Catalysis B: Environmental*, 6: 339–352.
- Nejar N, García-Cortés J M, Salinas-Martínez C L, Illán-Gómez M J, 2005. Bimetallic catalysts for the simultaneous removal of NO<sub>x</sub> and soot from diesel engine exhaust: A preliminary study using intrinsic catalysts. *Catalysis Communications*, 6: 263–267.
- Neri G, Rizzo G, Bonaccorsi L, Milone C, Galvagno S, 2005. Scale-up of sulphur resistant promoted-vanadium oxide catalysts for self-regenerating catalytic filters in off-road diesel engines and domestic apparatus. *Catalysis Today*, 100: 309–313.
- Peralta M A, Milt V G, Cornaglia L M, Querini C A, 2006. Stability of Ba, K/CeO<sub>2</sub> catalyst during diesel soot combustion: Effect of temperature, water, and sulfur dioxide. *Journal of Catalysis*, 242: 118–130.
- Russo N, Fino D, Saracco G, Specchia V, 2005. Studies on the redox properties of chromite perovskite catalysts for soot combustion. *Journal of Catalysis*, 229: 459–469.
- Teraoka Y, Kanada K, Kagawa S, 2001. Synthesis of La-K-Mn-O perovskite-type oxides and their catalytic property for simultaneous removal of NO<sub>x</sub> and diesel soot particulates. *Applied Catalysis B: Environmental*, 34: 73–78.
- Van S, Schouten J M, Makkee M, Moulijn J A, 2000. Realistic contact for soot with an oxidation catalyst for laboratory studies. *Applied Catalysis B: Environmental*, 28: 253–257.
- Wang Q, Park S Y, Duan L H, Chung J S, 2008. Activity, stability and characterization of NO oxidation catalyst Co/K<sub>x</sub>Ti<sub>2</sub>O<sub>5</sub>. *Applied Catalysis B: Environmental*, 85: 10–16.
- Wu X D, Liu D X, Li K, Li J, Weng D, 2007. Role of CeO<sub>2</sub>-ZrO<sub>2</sub> in diesel soot oxidation and thermal stability of potassium catalyst. *Catalysis Communications*, 8: 1274–1278.
- Zhang G Z, Zhao Z, Liu J, Xu J F, Jing Y N, Duan A J et al., 2009. Macroporous perovskite-type complex oxide catalysts of La<sub>1-x</sub>K<sub>x</sub>Co<sub>1-y</sub>Fe<sub>y</sub>O<sub>3</sub> for diesel soot combustion. *Journal of Rare Earth*, 27: 955–960.
- Zhang Y H, Zou X T, Sui L, 2006. The effects of potassium halides on catalytic activities of CeO<sub>2</sub>-K based catalysts for diesel soot oxidation. *Catalysis Communications*, 7: 855–859.
- Zhu L, Yu J J, Wang X Z, 2007. Oxidation treatment of diesel soot particulate on Ce<sub>x</sub>Zr<sub>1-x</sub>O<sub>2</sub>. *Journal of Hazardous Materials*, 140: 205–210.
- Zou Z Q, Meng M, Tsubaki N, He J J, Wang G, Li X G et al., 2009. Influence of Co or Ce addition on the NO<sub>x</sub> storage and sulfur-resistance performance of the lean-burn NO<sub>x</sub> trap catalyst Pt/K/TiO<sub>2</sub>-ZrO<sub>2</sub>. *Journal of Hazardous Materials*, 170: 118–126.